Comparison of the Structures of Three Carboxypeptidase A–Phosphonate Complexes Determined by X-ray Crystallography[†,‡]

Hidong Kim and William N. Lipscomb*
Gibbs Chemical Laboratory, Harvard University, Cambridge, Massachusetts 02138
Received March 12, 1991; Revised Manuscript Received May 13, 1991

ABSTRACT: The structures of the complexes of carboxypeptidase A (CPA) with two tight-binding phosphonate inhibitors have been determined by X-ray crystallography. The inhibitors, Cbz-Phe-Val^P-(O)-Phe[ZFV^P(O)F] and Cbz-Ala-Gly^P-(O)-Phe[ZAG^P(O)F], bind noncovalently to CPA with dissociation constants (K_i's) of 11 fM and 710 pM, respectively. The CPA–ZFV^P(O)F complex crystallizes in the space group $P2_12_12_1$ with unit cell parameters a = 65.3 Å, b = 63.4 Å, and c = 76.0 Å, and the CPA–ZAG^P(O)F complex crystallizes in the space group $P2_12_12_1$ with unit cell parameters a = 63.4 Å, b = 65.9 Å, and c = 74.4 Å. Both structures were determined by molecular replacement to a resolution of 2.0 Å. The final crystallographic residuals are 0.189 for the CPA–ZFV^P(O)F complex and 0.191 for the CPA–ZAG^P(O)F complex. The CPA–ZFV^P(O)F complex exhibits the lowest K_i yet determined for an enzyme–inhibitor interaction. Comparison of the CPA–ZFV^P(O)F structure with that of the CPA–ZAA^P(O)F complex [Kim, H., & Lipscomb, W. N. (1990) *Biochemistry 29*, 5546–5555] indicates the likely important contributions of hydrophobic and weakly polar enzyme–inhibitor interactions to the exceptional stability of the CPA–ZFV^P(O)F complex. Among these interactions is a network of four aromatic rings of CPA and ZFV^P(O)F in a configuration that allows stabilizing aromatic–aromatic edge-to-face interactions from one ring to the next. A comparison of the structures of the CPA–ZFV^P(O)F, CPA–ZAA^P(O)F and CPA–ZAG^P(O)F complexes shows that all three phosphonates assume a similar binding mode in the active-site binding groove of CPA. For ZAG^P(O)F, the glycyl P_1 residue does not lead to an anomalous or a partially disordered binding mode as seen in some previous complexes of CPA involving dipeptide analogue inhibitors with glycyl P_1 residues. The additional enzyme–inhibitor interactions for these tripeptide phosphonates secure a binding mode in which a P_i portion of the inhibitor is clearly bound by the corresponding S_i binding subsite. These three phosphonates have been implicated as transition-state analogues of the CPA-catalyzed reaction. The phosphinyl groups of these phosphonates coordinate to the active-site zinc in a manner that has been proposed as a characteristic feature of the general-base (Zn–hydroxyl or Zn–water) mechanism for the CPA-catalyzed reaction. Further mechanistic proposals are made for Arg-127, whose probable role in binding substrates is apparent in these CPA–phosphonate complexes.

Some recent studies on the zinc exoprotease carboxypeptidase A (CPA;[1] E.C. 3.4.17.1) have focused on its complexes with competitive phosphonate inhibitors (Hanson et al., 1989; Kim & Lipscomb, 1990). These extremely tight-binding inhibitors have been implicated as transition-state analogues of the general-base (Zn–hydroxyl or Zn–water) mechanism for the CPA-catalyzed reaction (Hanson et al., 1989; Kaplan & Bartlett, 1991). The crystal structure of one such CPA–phosphonate complex, involving the phosphonate Cbz-Ala-Ala^P-(O)Phe[ZAA^P-(O)F, Figure 1; K_i = 3 pM], has revealed structural features consistent with the transition-state analogy of these inhibitors and some unexpected enzyme–inhibitor interactions contributing to the great affinity of that complex (Kim & Lipscomb, 1990). Here, we report the crystal structures of the complexes of CPA with two other similar phosphonates, Cbz-Phe-Val^P-(O)Phe[ZFV^P(O)F, Figure 1; K_i = 11 fM] and Cbz-Ala-Gly^P-(O)Phe[ZAG^P(O)F, Figure 1; K_i = 710 pM].

CPA has been widely studied as a model system for understanding enzymatic catalysis and enzyme–inhibitor interactions. The study of an unprecedentedly tight-binding enzyme–inhibitor complex would be valuable in furthering our understanding of enzyme–inhibitor interactions. As one of our results in the present study, we report the binding mode of the phosphonate inhibitor Cbz-Phe-Val^P-(O)Phe to CPA as determined by X-ray crystallography. The K_i of 11 fM for the CPA–ZFV^P(O)F complex is the lowest yet measured for an enzyme–inhibitor interaction (Kaplan & Bartlett, 1991). It is more than 2 orders of magnitude lower than the K_i of any previous CPA complex studied by X-ray crystallography. Our study indicates that strongly polar enzyme–inhibitor interactions such as hydrogen bonds and salt links most likely do not account for this great differential stability. Rather, it appears that the extraordinary stability of this CPA complex is due largely to hydrophobic and weakly polar interactions.

The CPA–ZFV^P(O)F complex reported here is the second CPA–phosphonate structure determined. The binding mode of ZFV^P(O)F is very similar to that of ZAA^P(O)F, the structure of whose complex with CPA has previously been

[†] Support for this research was provided by a grant (GM-06920) to W.N.L. from the National Institutes of Health and a National Science Foundation predoctoral fellowship to H.K.

[‡] The coordinates for CPA–ZFV^P(O)F and CPA–ZAG^P(O)F have been submitted to the Brookhaven Protein Data Bank.

[1] Abbreviations: CPA, the zinc exoprotease carboxypeptidase A; ZFV^P(O)F, the phosphonate inhibitor of CPA Cbz-Phe-Val^P-(O)Phe; ZAA^P(O)F, the phosphonate inhibitor of CPA Cbz-Ala-Ala^P-(O)Phe; ZAG^P(O)F, the phosphonate inhibitor of CPA Cbz-Ala-Gly^P-(O)Phe; ZGP′, the phosphonamidate inhibitor of CPA Cbz-Gly^P-Phe; BOP, the ketonic inhibitor of CPA 5-benzamido-2-benzyl-4-oxopentanoic acid; ZG^{P}LL, the phosphonamidate inhibitor of thermolysin Cbz-Gly^P-Leu-Leu; ZF^{P}LA, the phosphonamidate inhibitor of thermolysin Cbz-Phe^P-Leu-Ala; rms, root mean square; F_o and F_c, observed and calculated structure factors. Full chemical names of the phosphonate inhibitors of CPA are given in the legend to Figure 1.

0006-2960/91/0430-8171$02.50/0

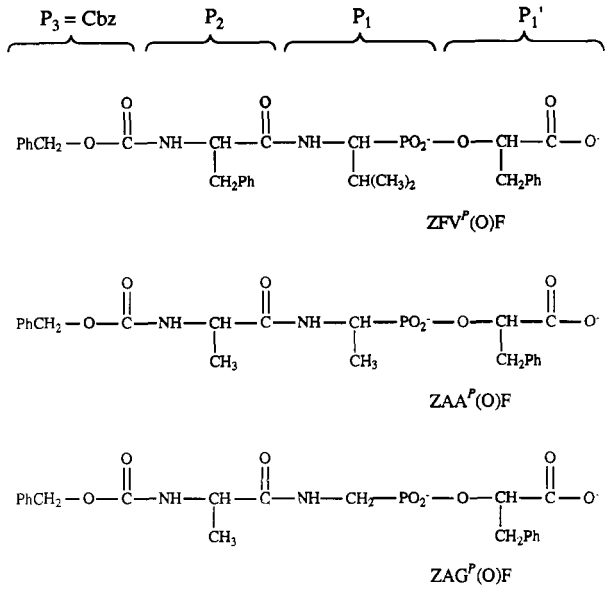

FIGURE 1: (From top to bottom) Tight-binding tripeptide phosphonate inhibitors of CPA: *O*-[[(1*R*)-[[*N*-(phenylmethoxycarbonyl)-L-phenylalanyl]amino]isobutyl]hydroxyphosphinyl]-L-3-phenyllactate [ZFV^P(O)F, K_i = 11 fM], *O*-[[(1*R*)-[[*N*-(phenylmethoxycarbonyl)-L-alanyl]amino]ethyl]hydroxyphosphinyl]-L-3-phenyllactate [ZAA^P(O)F, K_i = 3 pM], and *O*-[[(1*R*)-[[*N*-(phenylmethoxycarbonyl)-L-alanyl]amino]methyl]hydroxyphosphinyl]-L-3-phenyllactate [ZAG^P(O)F, K_i = 710 pM]. The residual portions of the inhibitors are indicated. In a true substrate, cleavage would occur at the P_1–P_1' linkage. Cbz = benzyloxycarbonyl.

determined (Kim & Lipscomb, 1990). In the present study, we also report the structure of a third CPA–phosphonate complex, involving the phosphonate Cbz-Ala-Gly^P-(O)Phe. It was speculated that because of its glycyl P_1 residue, ZAG^P-(O)F might not bind to CPA like ZAA^P(O)F and ZFV^P(O)F. Earlier studies on CPA showed that dipeptide substrates and inhibitors with glycyl P_1 residues exhibit both structural and kinetic anomalies (Christianson & Lipscomb, 1988; Christianson et al., 1987; Davies et al., 1968; Auld & Vallee, 1970). These anomalies are most likely due to the extra conformational freedom about the unsubstituted C_α of the glycyl P_1 residue. With no side chain to be held in the S_1 binding pocket and no enzyme–inhibitor interactions beyond the S_1 subsite to anchor the ligand, abnormal binding modes could arise, leading to the observed anomalies. For the CPA–ZAG^P(O)F complex, our study shows that in spite of its glycyl P_1 residue, ZAG^P(O)F assumes the normal binding mode as seen in ZAA^P(O)F, ZFV^P(O)F, and some other extended ligands. Enzyme–inhibitor interactions in the S_2 binding subsite and beyond appear to prevent undue rotation about the bonds to the glycyl P_1 C_α and thus secure the normal binding mode for ZAG^P(O)F.

These three CPA–phosphonate complexes share some other structural similarities, including the unusual cis conformation of the carbamoyl ester linkage between the P_3 and P_2 portions of the inhibitor. All three of these phosphonates have been implicated as transition-state analogues of the general-base mechanism for CPA-catalyzed hydrolysis (Hanson et al., 1989; Kaplan & Bartlett, 1991), and the structures of these CPA–phosphonate complexes show phosphinyl–zinc interactions that are consistent with the general-base mechanism. Also concerning the mechanism of CPA, all three complexes show the side chain of Arg-127 to be in a conformation that differs significantly from that of the native enzyme. This is a residue that is sometimes neglected in discussions of CPA. We believe that the structural results presented here are evidence for the importance of Arg-127 in the binding of substrates.

Materials and Methods

Crystals of the CPA–ZFV^P(O)F and CPA–ZAG^P(O)F complexes were grown under the same conditions as for the crystals of the CPA–ZAA^P(O)F complex (Kim & Lipscomb, 1990). Orthorhombic crystals of the two former complexes with dimensions 0.2 mm × 0.2 mm × 1.0 mm appeared within two weeks. Precession photographs identified the space group as $P2_12_12_1$ for both complexes with unit cell parameters a = 65.3 Å, b = 63.4 Å, and c = 76.0 Å for the CPA–ZFV^P(O)F complex and a = 63.4 Å, b = 65.9 Å, and c = 74.4 Å for the CPA–ZAG^P(O)F complex. There is one molecule of complex per asymmetric unit for each complex.

X-ray diffraction data were collected in the same manner as for the CPA–ZAA^P(O)F complex (Kim & Lipscomb, 1990). Data were collected from two crystals of each complex. For the CPA–ZFV^P(O)F complex, a total of 97 933 reflections to 2.0 Å, of which 21 226 were unique (97% completeness), was recorded. The 19 883 reflections between 10.0 and 2.0 Å with intensity greater than 2σ (91% completeness) were used in the refinement. The merging R [$R_{merge} = \sum_{hkl}(\sum_i|I - \bar{I}|/\sum_i I)$] for the data was 0.052. For the CPA–ZAG^P(O)F complex, a total of 93 048 reflections, of which 20 956 were unique (98% completeness), was collected to 2.0 Å. The 19 649 unique reflections (92% completeness) between 10.0 and 2.0 Å with intensity greater than 2σ were used in the refinement. The R_{merge} for the data was 0.053.

The apoenzyme of the CPA–ZAA^P(O)F complex (Kim & Lipscomb, 1990) was used as the initial model probe in the determination of the structures of the CPA–ZFV^P(O)F and the CPA–ZAG^P(O)F complexes. Rigid-body refinement of the CPA–ZAA^P(O)F apoenzyme against data from 7.0 to 5.0 Å produced crystallographic residuals [$R_{factor} = \sum_{hkl}(||F_o| - |F_c||/|F_o|)$] of 0.315 for the CPA–ZFV^P(O)F data and 0.309 for the CPA–ZAG^P(O)F data. The active-site zinc was added to the models, and after preliminary Powell minimization refinement, the enzyme portions of each complex were refined by simulated annealing refinement (Brünger et al., 1987; Brünger, 1988). The appropriate inhibitor and water molecules were then built into the electron density of the difference maps ($F_{complex} - F_{nat,calc}$) and the complexes were refined by Powell minimization and temperature factor refinement to final R_{factor}s of 0.189 for the CPA–ZFV^P(O)F complex and 0.191 for the CPA–ZAG^P(O)F complex. The CPA–ZFV^P(O)F structure contains 222 water molecules and the CPA–ZAG^P(O)F structure contains 254 water molecules. The rms deviations from ideal bond length and ideal bond angle are 0.013 Å and 2.9°, respectively, for both CPA–phosphonate structures.

For both the CPA–ZFV^P(O)F and CPA–ZAG^P(O)F sturctures, all model building was done on an Evans and Sutherland PS390 graphics system interfaced with a VAXstation 3200 using the program FRODO (Jones, 1982) and all refinements were executed with X-PLOR (Brünger et al., 1987; Brünger, 1988) on a DECstation 3100.

Results

One molecule of intact ZFV^P(O)F or ZAG^P(O)F occupies the active site of CPA. The binding modes of ZFV^P(O)F and ZAG^P(O)F are very much like that of ZAA^P(O)F (Figure 2, Tables I and II). Upon superposition of the coordinates of the enzyme C_α-chains of the CPA–ZAG^P(O)F complex and the CPA–ZFV^P(O)F complex onto the enzyme C_α-chain of the CPA–ZAA^P(O)F complex, there are only very small differences in the conformations of the inhibitor backbones (Figure 3). The rms difference in coordinates between the

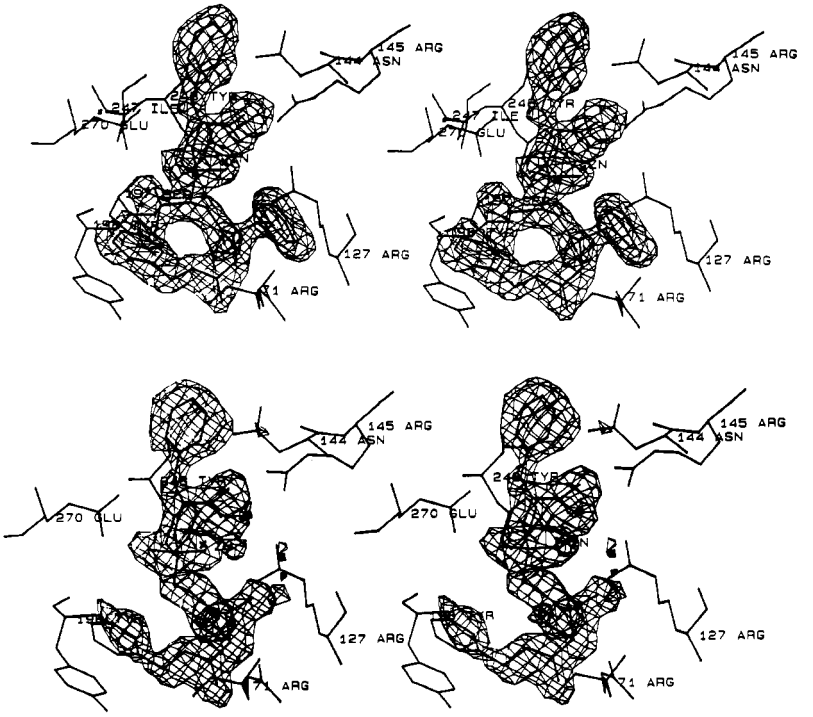

FIGURE 2: Stereoviews of $F_o - F_c$ maps showing the density of the bound ZFV^P(O)F (top) and the bound ZAG^P(O)F (bottom) in the active site of CPA. The contour level of the CPA–ZFV^P(O)F map is 3.0σ, and the contour level of the CPA–ZAG^P(O)F map is 2.7σ. The respective inhibitor was omitted from the structure factor calculations for each map. The coordinates of Arg-71, Arg-127, Asn-144, Arg-145, Ser-197, Tyr-198, Ile-247, Tyr-248, Glu-270, the zinc, and ZFV^P(O)F have been superimposed onto the CPA–ZFV^P(O)F map. The coordinates of Arg-71, Arg-127, Asn-144, Arg-145, Tyr-198, Tyr-248, Glu-270, the zinc, and ZAG^P(O)F have been superimposed onto the CPA–ZAG^P(O)F map.

Table I: Selected CPA–ZFV^P(O)F Interactions

enzyme atom	inhibitor atom	distance (Å)
Arg-145 $N_\eta 2$	carboxylate O2	3.5
Asn-144 $N_\delta 2$	carboxylate O1	3.1
Glu-270 $O_\epsilon 1$	phosphinyl O2	3.3
Glu-270 $O_\epsilon 2$	phosphinyl O2	2.4
Ser-197 O	phosphinyl O2	3.2
Arg-127 $N_\eta 1$	carboxylate O2	3.4
Arg-127 $N_\eta 2$	phosphinyl O1	2.8
Arg-127 $N_\eta 2$	phenylalanine O	3.1
Tyr-248 phenolic O	(O)phenylalanine O	3.3
Tyr-248 phenolic O	valine^P N	3.1
Arg-71 $N_\eta 1$	phenylalanine O	3.1
Zn	phosphinyl O2	3.0
Zn	phosphinyl O1	2.2

Table II: Selected CPA–ZAG^P(O)F Interactions

enzyme atom	inhibitor atom	distance (Å)
Arg-145 $N_\eta 1$	carboxylate O1	2.6
Arg-145 $N_\eta 1$	carboxylate O2	3.1
Asn-144 $N_\delta 2$	carboxylate O1	3.0
Glu-270 $O_\epsilon 1$	phosphinyl O2	3.1
Glu-270 $O_\epsilon 2$	phosphinyl O2	2.4
Ser-197 O	phosphinyl O2	3.2
Arg-127 $N_\eta 1$	carboxylate O2	3.2
Arg-127 $N_\eta 2$	phosphinyl O1	3.0
Arg-127 $N_\eta 2$	alanine O	2.7
Tyr-248 phenolic O	(O)phenylalanine O	3.1
Tyr-248 phenolic O	glycine^P N	3.2
Arg-71 $N_\eta 1$	alanine O	3.0
Zn	phosphinyl O2	3.2
Zn	phosphinyl O1	1.9

common atoms (the "backbone") of ZAG^P(O)F and ZFV^P-(O)F after superposition of their coordinates is 0.16 Å. The seven atoms of the Cbz benzyl portion of the inhibitors were excluded in this calculation since there is obviously a large difference in their coordinates. A similar comparison between ZAG^P(O)F and ZAA^P(O)F gives an rms deviation of 0.27 Å,

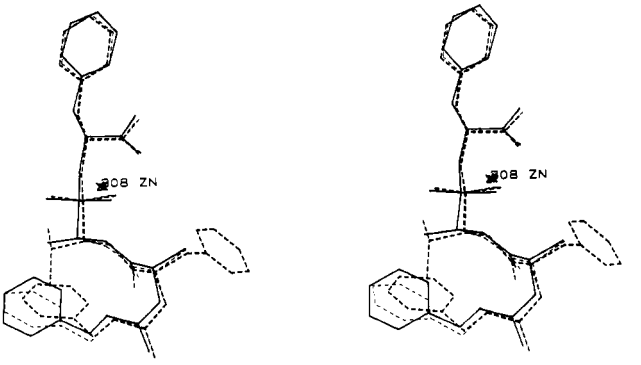

FIGURE 3: Stereoview of the coordinates of the CPA-bound ZAA^P(O)F (solid lines), ZFV^P(O)F (thick dashed lines), and ZAG^P(O)F (thin dashed lines) after the C_α-chains of the CPA–ZFV^P(O)F and CPA–ZAG^P(O)F complexes have been superimposed onto the C_α-chain of the CPA–ZAA^P(O)F complex. The zinc for each complex is also shown (308 is merely the designation of the zinc in the coordinate files).

and between ZAA^P(O)F and ZFV^P(O)F the difference is 0.22 Å.

At the active site, the phosphinyl groups of ZFV^P(O)F and ZAG^P(O)F are coordinated to the zinc in an orientation similar to that seen in the CPA–ZAA^P(O)F complex (Table III). The rotation of the phosphinyl group is toward Arg-127, albeit in the CPA–ZAG^P(O)F complex the coordination of the phosphinyl group to the zinc is more asymmetrical than in the other two CPA–phosphonate complexes. The difference in the two phosphinyl O–zinc distances is 0.8 Å in the CPA–ZFV^P(O)F complex and 0.9 Å in the CPA–ZAA^P(O)F complex. In the CPA–ZAG^P(O)F complex, this difference is 1.3 Å.

The molecular conformations of CPA in the CPA–ZFV^P-(O)F and the CPA–ZAG^P(O)F complexes show no significant changes from that of the native enzyme (Rees et al., 1983)

Table III: Phosphinyl Oxygen–Zinc Interactions[a]

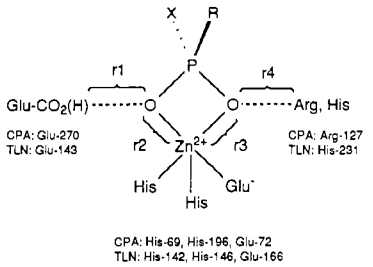

enzyme	inhibitor	X	*r*1	*r*2	*r*3	*r*4	reference
CPA	ZGP′[b]	NHR′	2.6	2.4	3.5	2.6	Christianson and Lipscomb (1988)
CPA	ZAG^P(O)F	OR′	2.4	3.2	1.9	3.0	this work
CPA	ZAA^P(O)F	OR′	2.2	3.1	2.2	2.8	Kim and Lipscomb (1990)
CPA	ZFV^P(O)F	OR′	2.4	3.0	2.2	2.8	this work
TLN	phosphoramidon	NHR′	2.5	3.4	1.8	3.2	Tronrud et al. (1986)
TLN	ZG^{P}LL	NHR′	2.5	3.0	2.1	2.9	Holden et al. (1987)
TLN	ZF^{P}LA	NHR′	2.3	2.6	2.2	2.7	Holden et al. (1987)

[a] All distances are given in angstroms. [b] Evidence of transition-state analogy for ZGP′, a phosphonamidate inhibitor of CPA, is much less certain than that for the phosphonate inhibitors of CPA and the phosphonamidate inhibitors of thermolysin (Jacobsen & Bartlett, 1981; Bartlett & Marlowe, 1983, 1987; Hanson et al., 1989). Note that the phosphinyl group of ZGP′ is rotated in the opposite direction compared with the other inhibitors.

or the CPA–ZAA^P(O)F complex (Kim & Lipscomb, 1990). The rms deviation in coordinates between the enzyme backbone of the CPA–ZFV^P(O)F or the CPA–ZAG^P(O)F complex and that of the other three structures in less than 0.4 Å. Furthermore, the crystal packings of all three CPA–phosphonate complexes are very similar. The small differences in the unit cell lengths of these three CPA–phosphonate complexes are likely due to subtle structural changes in each particular complex resulting from enzyme–inhibitor and solvent interactions.

Discussion

CPA–ZFV^P(O)F Complex. The most intriguing of the three CPA–phosphonate complexes discussed here is the one involving the phosphonate inhibitor Cbz-Phe-Val^P-(O)Phe-[ZFV^P(O)F, Figure 1]. With a K_i of 11 fM, this complex is the strongest enzyme–inhibitor interaction yet determined, being only 1 order of magnitude less tightly bound than the biotin–avidin complex (Green, 1963; Kaplan & Bartlett, 1991). The structure of the CPA–ZFV^P(O)F complex is very similar to that of the CPA–ZAA^P(O)F complex, which has a K_i of 3 pM (Kim & Lipscomb, 1990). Because the hydrogen bonds and salt links seen in these two complexes are so similar (Table I), it is likely that these strongly polar enzyme–inhibitor interactions are not the chief reason for the more than 2 orders of magnitude greater stability of the CPA–ZFV^P(O)F complex (Hanson et al., 1989; Kaplan & Bartlett, 1991).

Since the difference between ZAA^P(O)F and ZFV^P(O)F is the additional set of nonpolar side chains in the latter, the great difference in binding constants for the two inhibitors is likely due in large part to nonpolar enzyme–inhibitor interactions and hydrophobic effects involving these side chains.[2] In the S_1 subsite, the side chain of the valine^P portion of ZFV^P(O)F is bound in the pocket formed by Ser-197, Tyr-198, Ile-247, Tyr-248, and Glu-270. One can expect stabilization when alanine^P in ZAA^P(O)F is replaced with valine^P in ZFV^P(O)F in the S_1 hydrophobic pocket due to the greater hydrophobicity of the valine side chain. The free energy of transfer from water to ethanol for valine is 1.0 kcal/mol more favorable than that for alanine (Nozaki & Tanford, 1971). Also, in comparison with the alanine side chain, space-filling models show that the valine side chain fills this binding pocket particularly well (Figure 4). Bartlett has demonstrated the much tighter binding of tripeptide phosphonates by the single substitution of a P_1 alanine^P with a valine^P (Kaplan & Bartlett, 1991). As a measure of the more extensive fit of the valine side chain in the P_1 binding pocket compared with the alanine side chain, the solvent-accessible surface areas of the enzyme residues shown in Figure 3 were calculated for the CPA–ZFV^P(O)F and CPA–ZAA^P(O)F complexes using the algorithm of Lee and Richards (1971). With respect to a spherical solvent molecule with a radius of 1.6 Å, this pocket has 124 Å^2 of accessible surface area in the CPA–ZAA^P(O)F complex and only 90 Å^2 of accessible surface area in the CPA–ZFV^P(O)F complex. Most of this decrease in accessible surface area is seen in Ile-247 and Tyr-248. In the CPA–ZFV^P(O)F complex, the side chain of Ile-247 moves toward the valine side chain of ZFV^P(O)F in order to make this enzyme–inhibitor interaction. This movement of the Ile-247 side chain also brings it into closer contact with the phenol side chain of Tyr-248.

In the S_2 subsite and beyond, the aromatic side chains of the P_2 and P_3 portions of ZFV^P(O)F are within van der Waals distance of the aromatic side chains of Tyr-198 and Tyr-248. The geometries of these enzyme–inhibitor aromatic–aromatic interactions show that the phenyl rings of the inhibitor and the phenol rings of the enzyme make enthalpically favorable aromatic–aromatic edge-to-face interactions. These spatially anisotropic weakly polar interactions afford stabilization, beyond van der Waals interactions, by the interaction of the slightly positiviely charged edge of one aromatic ring with the slightly negatively charged face of a second aromatic ring (Burley & Petsko, 1985, 1986, 1988). Thus, a particular configuration of two aromatic rings in a stabilizing edge-to-face configuration will give specific additional stabilization in addition to the usual induced and fluctuating multipoles. What is especially interesting about the edge-to-face interactions seen in this complex is that the aromatic rings are oriented such that these stabilizing interactions extend from one pair of aromatic rings to the next (Figure 5, Table IV). These enzyme–inhibitor edge-to-face interactions form a continuous network of interactions rather than being merely isolated pairs

[2] It is also possible that, because of its larger nonpolar side chains, ZFV^P(O)F interacts less well with the aqueous solvent than does ZAA^P(O)F when the inhibitors are not bound to the enzyme. Our analysis neglects this effect, the magnitude of which is unknown.

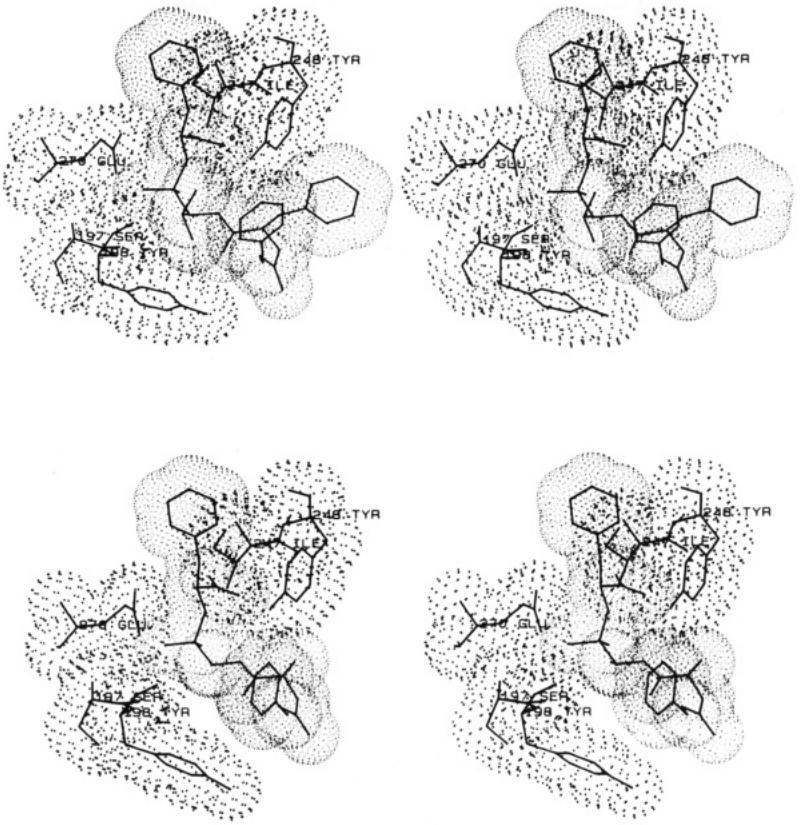

FIGURE 4: Stereoviews of space-filling models of the S_1 subsite in the CPA–ZFV^P(O)F complex (top) and the CPA–ZAA^P(O)F complex (bottom). The van der Waals volumes of Ser-197, Tyr-198, Ile-247, Tyr-248, and Glu-270 are shown in coarse stippling. The van der Waals volumes of the inhibitors are shown in fine stippling.

Table IV: Aromatic–Aromatic Edge-to-Face Geometries[a] and Interaction Energies[b]

aromatic pair	r (Å)	θ (deg)	IA (deg)	E_{nb}
Tyr-198–Cbz[c]	6.6	49	42	−0.8
Cbz–Tyr-248[c]	5.7	35	78	−1.6
Tyr-248–Phe[c]	5.8	37	70	−1.3
Tyr-198–Cbz[d]	5.8	38	90	−0.7
Cbz–Tyr-248[d]	6.7	81	58	−0.8
Tyr-198–Cbz[e]	4.8	37	50	0.8
Cbz–Tyr-248[e]	6.6	77	82	−0.7

[a] Geometric parameters defined by Burley and Petsko (1986). IA = interplanar angle. [b] E_{nb} is the nonbonded potential energy of two benzene rings in the same configuration as the aromatic pair indicated, calculated from the model of Karlström et al. (1983). [c] CPA–ZFV^P(O)F complex. [d] CPA–ZAA^P(O)F complex (Kim & Lipscomb, 1990). [e] CPA–ZAG^P(O)F complex.

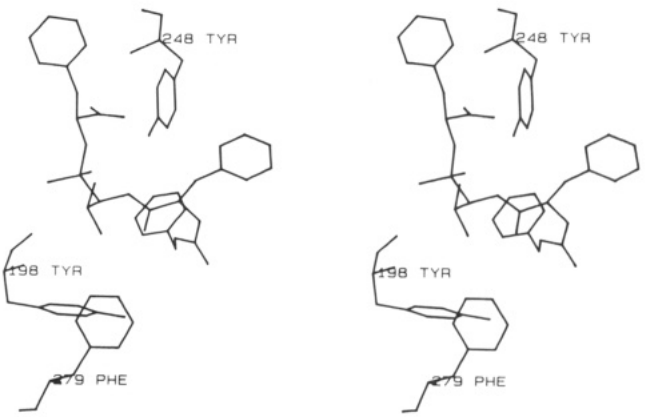

FIGURE 5: Stereoview of the coordinates of Tyr-198, Tyr-248, Phe-279, and ZFV^P(O)F in the CPA–ZFV^P(O)F complex showing the aromatic–aromatic edge-to-face network.

of interacting rings. Furthermore, the phenyl ring of Phe-279 of the enzyme is involved in a stabilizing edge-to-face interaction with the phenol ring of Tyr-198 (but not with the inhibitor) in both the native enzyme and in the complex. If Phe-279 is included, the aromatic–aromatic edge-to-face network extends over five aromatic rings. Networks of this kind occur in hydrophobic regions of many macromolecules (Burley & Petsko, 1985, 1986, 1988).

In order to estimate the contribution of these hydrophobic and weakly polar enzyme–inhibitor interactions to the stability of the CPA–ZFV^P(O)F complex, we examined the differences in the enzyme–inhibitor interaction energies between this and the CPA–ZAA^P(O)F complex due to the substitution of P_1 and P_2 alanine residues in ZAA^P(O)F with valine and phenylalanine, respectively, in ZFV^P(O)F. The binding affinity of an inhibitor for an enzyme depends on the change in the free energy between the enzyme and inhibitor in solution and the enzyme–inhibitor complex. This change in free energy that accompanies enzyme–inhibitor association can be divided approximately into two terms. The first is the free energy of transfer of the inhibitor from the aqueous solvent environment to the more hydrophobic protein environment of the enzyme. This transfer from water to protein was modeled by the transfer from water to ethanol. The differences in the free energies of transfer from water to ethanol have been measured to be 1.0 kcal/mol between the valine and alanine side chains and 2.0 kcal/mol between the phenylalanine and alanine side chains (Nozaki & Tanford, 1971).[3] The value for the transfer free energy difference between valine and alanine seems ap-

[3] In this reference, the transfer free energy given for phenylalanine is the average of values for the transfers from water to ethanol and from water to dioxane.

propriate for this analysis since both the P_1 valine side chain of $ZFV^P(O)F$ and the P_1 alanine side chain of $ZAA^P(O)F$ are deeply buried in the S_1 hydrophobic pocket in their respective complexes. The value for the transfer free energy difference between phenylalanine and alanine is most likely too high for this analysis since the P_2 phenylalanine side chain is still quite exposed to the aqueous solvent in the CPA-$ZFV^P(O)F$ complex. The small difference between the K_i's of Cbz-Ala-Ala^P-(O)Phe (3 pM) and Cbz-Phe-Ala^P-(O)Phe (1 pM) (Hanson et al., 1989) seems to indicate that the P_2 phenylalanine side chain is relatively unimportant in the affinity of the CPA–phosphonate complexes. On the basis of the structures of the CPA–$ZAA^P(O)F$, CPA–$ZFV^P(O)F$, and CPA–$ZAG^P(O)F$ complexes, we believe that tripeptide phosphonates bind similarly to CPA. Therefore, although the structure of the CPA–$ZFA^P(O)F$ complex is not known, it is likely that the P_2 phenylalanine side chain of $ZFA^P(O)F$ and other such tripeptide phosphonates are, as in $ZFV^P(O)F$, rather uninvolved in enzyme–inhibitor contacts.

The second term contributing to the change in free energy upon enzyme–inhibitor association involves localized enzyme–inhibitor interactions. We specifically considered the aromatic–aromatic enzyme–inhibitor interactions in these two complexes, which we modeled with benzene molecules. The nonbonded potential energies of interacting benzenes in the same configuration as the interacting aromatic rings in the CPA–$ZFV^P(O)F$ and the CPA–$ZAA^P(O)F$ complex were calculated using the model of Karlström et al. (1983) (Table IV). These calculations show that a benzene model of the CPA–$ZFV^P(O)F$ interaction is more stable than a corresponding model of the CPA–$ZAA^P(O)F$ interaction by 2.2 kcal/mol.

Although the energetic effects described in the previous two paragraphs cannot be quantitatively combined due to the neglect of entropic terms in the calculation of the aromatic–aromatic interaction energies, the magnitude of these effects is consistent with tighter binding for the CPA–$ZFV^P(O)F$ complex over the CPA–$ZAA^P(O)F$ complex (Hanson et al., 1989; Kaplan & Bartlett, 1991). Notwithstanding the approximations, it seems clear that these hydrophobic and weakly polar enzyme–inhibitor interactions contribute significantly to the extraordinary stability of the CPA–$ZFV^P(O)F$ complex.

Phosphonate Binding Mode. $ZFV^P(O)F$ is just one of several tripeptide phosphonates that have been shown to be extremely potent competitive inhibitors of CPA (Hanson et al., 1989; Kaplan & Bartlett, 1991). The CPA complexes involving $ZAG^P(O)F$, $ZAA^P(O)F$, and $ZFV^P(O)F$ have K_i's lower than that of any previous CPA complex of known structure. Before the work on phosphonates, the 5 nM CPA–potato inhibitor complex was the tightest-binding CPA complex of known structure (Rees & Lipscomb, 1982). The 39-amino acid potato inhibitor was somewhat unusual in the history of CPA–ligand studies due to its great size. The high affinity of that complex was largely attributed to the size of the potato inhibitor, which made possible many enzyme–inhibitor contacts. More commonly, dipeptides and their analogues, usually with a glycyl P_1 residue, had been used in CPA–ligand studies (Snoke & Neurath, 1949; Davies et al., 1968).[4] Certainly, one of the reasons for the much greater affinity of the tripeptide phosphonates over dipeptide inhibitors with binding constants in the millimolar to micromolar range is that the increased length of these phosphonates provides more opportunities for CPA–inhibitor interactions. Enzyme–inhibitor interactions involving the P_2 amino acid and the P_3 benzyloxycarbonyl of the inhibitor are seen in the CPA–$ZAA^P(O)F$ and CPA–$ZFV^P(O)F$ complexes. One of these interactions is a hydrogen bond between the P_2 carbonyl oxygen of the inhibitor and a guanidinium nitrogen of Arg-71.

Crystallographic studies of CPA–dipeptide analogue complexes with a glycyl P_1 residue have shown partially disordered or anomalous binding at the N-terminus of the inhibitor (Christianson & Lipscomb, 1988; Christianson et al., 1987). This is most likely due to the conformational freedom about the C_α of the glycyl P_1 residue. Anomalous binding of glycyl P_1 inhibitors has also been seen in complexes of thermolysin, a zinc protease similar to CPA. The phosphonamidate inhibitor Cbz-Gly^P-Leu-Leu binds to thermolysin with its benzyloxycarbonyl group rotated more than 100° about the P_1 N–C_α bond, relative to a more normal binding phosphonamidate inhibitor (Holden et al., 1987; Bartlett & Marlowe, 1983, 1987). Because of the anomalous binding seen in these CPA and thermolysin complexes, all involving inhibitors with a glycyl P_1 residue, it seemed possible that $ZAG^P(O)F$, with its glycyl P_1 residue, might assume an appreciably different binding mode than $ZAA^P(O)F$ and $ZFV^P(O)F$. The results of our present X-ray crystallographic determination of the CPA-$ZAG^P(O)F$ structure show clearly that the binding mode of $ZAG^P(O)F$ is very similar to that of $ZAA^P(O)F$ and $ZFV^P(O)F$ (Figures 2 and 3). There is very little conformational deviation in the backbones of these three bound inhibitors, even at the P_1 residue (Figure 3). The enzyme–inhibitor interactions at the S_2 subsite and beyond, most notably the hydrogen bond between the P_2 carbonyl O and Arg-71, appear to attenuate the conformational freedom of the glycyl P_1 residue and hold $ZAG^P(O)F$ in the more normal binding mode as seen in the other extended phosphonate inhibitors, $ZAA^P(O)F$ and $ZFV^P(O)F$.

This normal binding mode was also seen in the complex of CPA with a hydrated ketomethylene substrate analogue (Shoham et al., 1988). This inhibitor is a dipeptide analogue with an N-terminal *tert*-butoxycarbonyl blocking group and a phenylalanyl P_1 residue. The combination of the carbonyl of the blocking (P_2) group hydrogen-bonded to Arg-71 and the P_1 phenylalanyl side chain anchored in the S_1 hydrophobic pocket kept this dipeptide inhibitor in the normal binding mode whereas some other dipeptide inhibitors of CPA bound anomalously (Christianson & Lipscomb, 1988; Christianson et al., 1987). While a P_2 carbonyl O–Arg-71 interaction is present in all CPA–ligand complexes exhibiting the normal binding mode, the potential for this particular interaction does not ensure a normal binding mode for a ligand. The ketonic substrate analogue BOP and the phosphonamidate inhibitor ZGP′ both have a glycyl P_1 residue and a carbonyl of an N-terminal blocking group that could conceivably interact with Arg-71. However, the N-terminal benzamido portion of BOP was partially disordered and the N-terminal benzyloxycarbonyl portion of ZGP′ was anomalously bound in the S_1 hydrophobic pocket (Christianson & Lipscomb, 1988; Christianson et al., 1987). No enzyme–inhibitor interactions involving Arg-71 were seen for either inhibitor. In the case of BOP, there was no P_1 side chain to fill the S_1 binding pocket. The lack of a side-chain anchor in the S_1 subsite appears to contribute to the disordered binding in the N-terminal region of BOP. For ZGP′, although there was no P_1 side chain, the phenyl side chain of the benzyloxycarbonyl group was anomalously bound in the S_1 hydrophobic pocket. It appears that the complex has favored filling the S_1 pocket over the carbonyl–Arg-71 in-

[4] It should be noted that more recent studies have examined tripeptide analogues and other extended ligands (Galdes et al., 1983, 1986; Geoghegan et al., 1983, 1986; Auld et al., 1984).

teraction. The importance of nonpolar enzyme–inhibitor interactions in the affinity of CPA complexes has been demonstrated above with the CPA–ZAA^P(O)F and CPA–ZFV^P(O)F complexes. The absence of such a hydrophobic interaction in the S_1 pocket of the CPA–ZAG^P(O)F complex is very likely a factor in the lower affinity of this complex compared with the other two CPA–phosphonate complexes. Also, a recent NMR study of thermolysin–phosphonamidate complexes suggests that the much tighter binding of Cbz-Phe^P-Leu-Ala (K_i = 0.068 nM) over Cbz-Gly^P-Leu-Ala (K_i = 16.5 nM) is probably due to the increased hydrophobic interactions in the former complex (Copié et al., 1990).

All three phosphonates, ZAG^P(O)F, ZAA^P(O)F, and ZFV^P(O)F, a show a cis carbamoyl ester linkage between their P_3 and P_2 portions. The cis conformation of the carbamoyl ester linkage allows the phenyl ring of the P_3 Cbz group to make favorable aromatic–aromatic interactions (Burley & Petsko, 1985, 1986, 1988) with the phenol rings of Tyr-198 and Tyr-248. Originally, it was speculated that this carbamoyl ester linkage was involved in the modest increase in the on-rate for the binding of ZAG^P(O)F compared with phosphonates with α-substituted P_1 residues (Kim & Lipscomb, 1990). The hypothesis was that the increased conformational freedom about the glycyl P_1 residue of ZAG^P(O)F would make possible a binding mode that did not require a cis carbamoyl ester bond, and therefore, the binding of ZAG^P(O)F could bypass a potentially slow trans to cis interconversion of the carbamoyl ester bond. It is now clear that ZAG^P(O)F binds similarly to α-substituted P_1 phosphonates, as the electron density around the carbamoyl ester linkage of ZAG^P(O)F shows the cis conformation. Thus, the differences between the on-rates of ZAG^P(O)F and α-substituted P_1 phosphonates (Hanson et al., 1989) are not due to cis vs trans carbamoyl ester linkages between these inhibitors. More likely, the faster on-rate for ZAG^P(O)F is due to its less bulky side chains.

The normal binding mode for CPA ligands has now been seen in the complexes of CPA with the tripeptide phosphonates ZAG^P(O)F, ZAA^P(O)F (Kim & Lipscomb, 1990), and ZFV^P(O)F, a dipeptide ketomethylene (Shoham et al., 1988), and in the three C-terminal residues of the potato inhibitor (Rees & Lipscomb, 1982). It is very likely that this binding mode is a characteristic feature of tripeptide phosphonate inhibitors. This binding mode, partially characterized by the P_2 carbonyl O–Arg-71 interaction, is most likely also the productive binding mode for polypeptide substrates of CPA. Many earlier kinetic studies of CPA have focused on dipeptide analogue substrates with glycine at the P_1 position (Snoke & Neurath, 1949; Davies et al., 1968). The CPA-catalyzed hydrolyses of such dipeptide analogue substrates show deviations from classical Michaelis–Menten kinetics, whereas tripeptide substrates do not show these kinetic anomalies (Abramowitz et al., 1967; Auld & Vallee, 1970). It has also been observed that the tripeptide substrate Cbz-Gly-Gly-Phe has a K_m one-fourth that of the "classical" dipeptide substrate Cbz-Gly-Phe (Abramowitz et al., 1967). These results suggest that tripeptides are better substrates for CPA than dipeptides. Tripeptides (and other extended ligands) are likely better suited for modeling the polypeptide substrates of CPA encountered in digestion. We suggest that the an important factor behind the observed kinetic differences between glycyl P_1-containing dipeptide substrates and more extended substrates is the significantly different binding modes between these two classes of substrates. Others have previously made such a proposition (Auld & Vallee, 1970). The results of our present crystallographic study provide structural evidence of these different binding modes and strengthen this hypothesis. The substrates of CPA that exhibit Michaelis–Menten kinetics most likely bind to CPA in the normal binding mode as seen in the present CPA–phosphonate complexes, while for glycyl P_1-containing dipeptide substrates, their conformational freedom makes possible anomalous or disordered binding modes.

CPA also hydrolyzes esters, and studies of the esterolytic activity of CPA have raised questions regarding the mechanistic similarity between CPA-catalyzed proteolysis and esterolysis (Makinen et al., 1979; Galdes et al., 1983, 1986; Geoghegan et al., 1983). Whether or not these two reactions proceed by the same mechanism, it appears that di- and tridepsipeptide substrates of CPA show similar kinetic effects as their analogous peptide substrates. The didepsipeptide benzoyl-Gly-L-(O)Phe shows kinetic anomalies at high substrate concentrations, while longer depsipeptide substrates show classical Michaelis–Menten kinetics over a wide range of substrate concentration (Auld & Holmquist, 1974). As is proposed for peptide substrates, such kinetic differences between didepsipeptide and more extended depsipeptide substrates are likely due to differences in their binding modes.

Although there are no crystal structures of CPA–intact extended substrate complexes, the structure of the complex of CPA with the slowly hydrolyzed substrate *N*-benzoyl-L-phenylalanine may depict the features of a normal binding substrate (Christianson & Lipscomb, 1987). The observed structure of this complex is very likely an enzyme–substrate–product complex for the hydrolysis of *N*-benzoyl-L-phenylalanyl-L-phenylalanine. It can also be interpreted as the Michaelis complex of the reverse, synthetic reaction. This complex shows the important characteristic features of the normal binding mode, namely, the P_1 (phenyl) side chain anchored in the S_1 binding pocket and a hydrogen bond between the P_2 carbonyl of the ligand and Arg-71.

The dipeptide analogues discussed thus far have been N-blocked species. Peptide substrates with free N-termini have also been examined by several workers. As with N-blocked substrates, substrates with free N-termini show structural and kinetic anomalies between dipeptide and longer peptide species. The crystal structure of the complex of CPA with the slowly hydrolyzed substrate Gly-L-Tyr showed that the free amino group of the N-terminal glycine was coordinated to the active-site zinc (Izumiya & Uchio, 1959; Lipscomb et al., 1968; Rees et al., 1981; Christianson & Lipscomb, 1986). The chelation of the substrate, via its N-terminal amino and scissile carbonyl groups, to the zinc was proposed as a characteristic feature of the binding mode of dipeptides with free amino termini, which are generally slowly hydrolyzed by CPA (Hofmann & Bergmann, 1940; Fu et al., 1954; Yanari & Mitz, 1957). Adding a glycine, however, to the N-terminus of the slowly hydrolyzed substrate L-Leu-L-Tyr resulted in a dramatic increase in the rate of hydrolysis (Yanari & Mitz, 1957). Furthermore, Gly_2-L-Tyr is hydrolyzed nearly 200 times faster than Gly-L-Tyr, while the hydrolytic rates of Gly_n-L-Tyr (n = 2–5) are very similar to each other (Izumiya & Uchio, 1959). This very sharp discrepancy in the hydrolysis rates between dipeptides and longer peptides with free N-termini is very likely attributable in great part to differences in the binding modes of these substrates. Whereas the P_1 amino group of a free N-terminal dipeptide binds to the zinc, the P_1 amino group of a longer free N-terminal peptide is most likely bound by the phenol O of Tyr-248 as in the normal binding mode of the CPA–phosphonate complexes. By coordinating to the zinc, the N-terminal amino group of an unblocked dipeptide would hinder the electrophilic activation

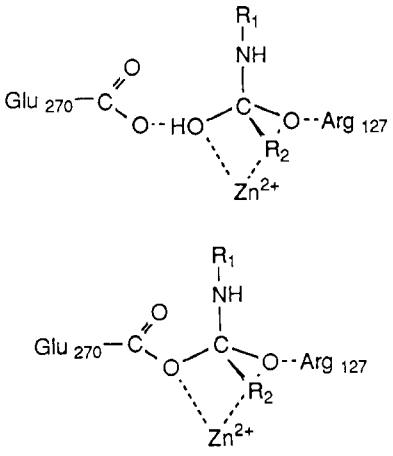

FIGURE 6: Tetrahedral carbon intermediates formed in the general-base (top) and acyl (bottom) mechanisms for CPA-catalyzed hydrolysis. Covalent bonds are represented by solid lines and hydrogen bonds are represented by dashed lines.

of water by the zinc and thus impede catalysis.

Mechanism of Catalysis. ZAG^P(O)F, ZAA^P(O)F, and ZFV^P(O)F have all been implicated as transition-state analogue inhibitors of the CPA-catalyzed reaction (Hanson et al., 1989; Kaplan & Bartlett, 1991). Thus, one aspect of the extremely tight-binding nature of these inhibitors is that they are good models of the transition state of the CPA-catalyzed reaction, and as such, they are models of the transition state of the proposed general-base mechanism for CPA (Pauling, 1948; Lienhard, 1973; Wolfenden, 1976; Christianson & Lipscomb, 1989). There is some debate over whether the CPA-catalyzed reaction proceeds through a gem-diolate or a covalent acyl enzyme intermediate (Figure 6). The transition-state analogy, which was directly shown for several tripeptide phosphonate inhibitors of CPA, is strong evidence for the gem-diolate intermediate and thus the general-base mechanism for CPA, since these inhibitors cannot effectively model the covalent intermediate of the acyl mechanism (Hanson et al., 1989).

There are structural features in the CPA complexes involving ZAG^P(O)F, ZAA^P(O)F, and ZFV^P(O)F that are consistent with the general-base mechanism. The phosphinyl–zinc interactions in all three complexes are similar to those seen in complexes of thermolysin with phosphonamidate transition-state analogues (Table III). Thermolysin is a zinc endoprotease with an arrangement of active-site residues similar to that in CPA, and the general-base mechanism is firmly accepted for the thermolysin-catalyzed reaction (Matthews, 1988). In the CPA–phosphonate and thermolysin–phosphonamidate complexes, the phosphinyl group, which is the characteristic transition-state-mimicking moiety, is rotated toward the active-site electrophile (Arg-127 in CPA, His-231 in thermolysin), viewing down the active site from S_1 to S_1'. This particular rotation of the phosphinyl group (or gem-diolate) may be a characteristic feature of the transition states of the CPA- and themolysin-catalyzed reactions.

The strength of binding increases dramatically from ZAG^P(O)F to ZAA^P(O)F to ZFV^P(O)F[5] and may be partially reflected in the specifics of their phosphinyl–zinc interactions. From ZAG^P(O)F to ZAA^P(O)F, there is more than 2 orders of magnitude tighter binding and we see a more bidentate phosphinyl–zinc interaction for ZAA^P(O)F but not much shorter phosphinyl O–zinc distances. The more symmetrical phosphinyl–zinc coordination in the CPA–ZAA^P(O)F complex likely contributes to the greater stability of that complex. Although ZFV^P(O)F binds more than 2 orders of magnitude more tightly than ZAA^P(O)F, there is very little difference in the geometry of the phosphinyl–zinc interaction between these two complexes. Thus, this interaction probably does not contribute much to the greater stability of the CPA–ZFV^P(O)F complex. As already discussed, hydrophobic and weakly polar enzyme–inhibitor interactions are probably most important in the large difference between the stabilities of the CPA–ZFV^P(O)F and the CPA–ZAA^P(O)F complexes. The transition state in the general-base mechanism of the CPA-catalyzed reaction is presumed to have the gem-diolate oxygens of the tetrahedral carbon bound to zinc in a progression of orientations that at some stage may involve bidentate coordination (Christianson & Lipscomb, 1988). The 0.8-Å difference in the phosphinyl O–zinc distances seen in the CPA–ZFV^P(O)F complex may be close to the limit of bidenticity for the gem-diolate oxygen–zinc distances in the CPA-catalyzed reaction. This claim must be made with some caution since phosphinyl–metal interactions are electronically predisposed toward asymmetrical coordination (Alexander et al., 1990). Nevertheless, for one thermolysin–phosphonamidate complex, the difference in the oxygen–zinc distances in the phosphinyl–zinc interaction has been reported to be as small as 0.4 Å (Holden et al., 1987).

The conformation of Arg-127 in these three CPA–phosphonate complexes appears to confirm an important role for this residue in the CPA-catalyzed reaction. That Arg-127 has a role in the binding of substrates was first proposed on the basis of the crystal structure of the apo-CPA–Gly-L-Tyr complex (Rees & Lipscomb, 1983). The first indication of a binding role for Arg-127 in the holoenzyme came from the crystal structure of a CPA–hydrated aldehyde complex (Christianson & Lipscomb, 1985). In that complex, the guanidinium NH units of Arg-127 approached both the terminal carboxylate and one of the hydrate oxygens of the inhibitor. Also, a recent study on rat carboxypeptidase A1 indicates that Arg-127 is important in stabilizing the transition state of the CPA-catalyzed reaction while playing a lesser role in the binding of the ground-state substrate. Site-directed mutagenesis and electrostatic calculations show that, in rat carboxypeptidase A1, Arg-127 acts as an electrophile in stabilizing the oxyanionic tetrahedral intermediate [Phillips et al., 1990; for a review of the mechanism, see Christianson and Lipscomb (1989)]. In the three CPA–phosphonate complexes, Arg-127 clearly interacts with the terminal carboxylate and one of the phosphinyl oxygens of the phosphonate. These contacts induce an extended conformation in the Arg-127 side chain different from that seen in the native enzyme. There is a small displacement (0.3 Å) in the position of the $N_\eta 2$ guanidinium nitrogen, which interacts with a phosphinyl oxygen of the phosphonate, and a large displacement (2 Å) in the position of the $N_\eta 1$ guanidinium nitrogen, which interacts with the terminal carboxylate. This elongated conformation of the Arg-127 side chain is not seen in all CPA complexes (Figure 7). It is seen in complexes involving transition-state and reaction-coordinate analogues. The coiled conformation of the Arg-127 side chain, like that in the native enzyme, is seen in some complexes involving less productively bound

[5] It may be tempting to say that, along with the stability of the CPA–phosphonate complex, the transition-state analogy for the CPA reaction also increases from ZAG^P(O)F to ZAA^P(O)F to ZFV^P(O)F. However, it would be imprudent to say that one phosphonate (or any one molecule) is a better transition-state analogue than another in a general sense. On the basis of the work of Bartlett (Hanson et al., 1989), we can only say that these tripeptide phosphonates are good transition-state analogues for their particular corresponding peptide substrates.

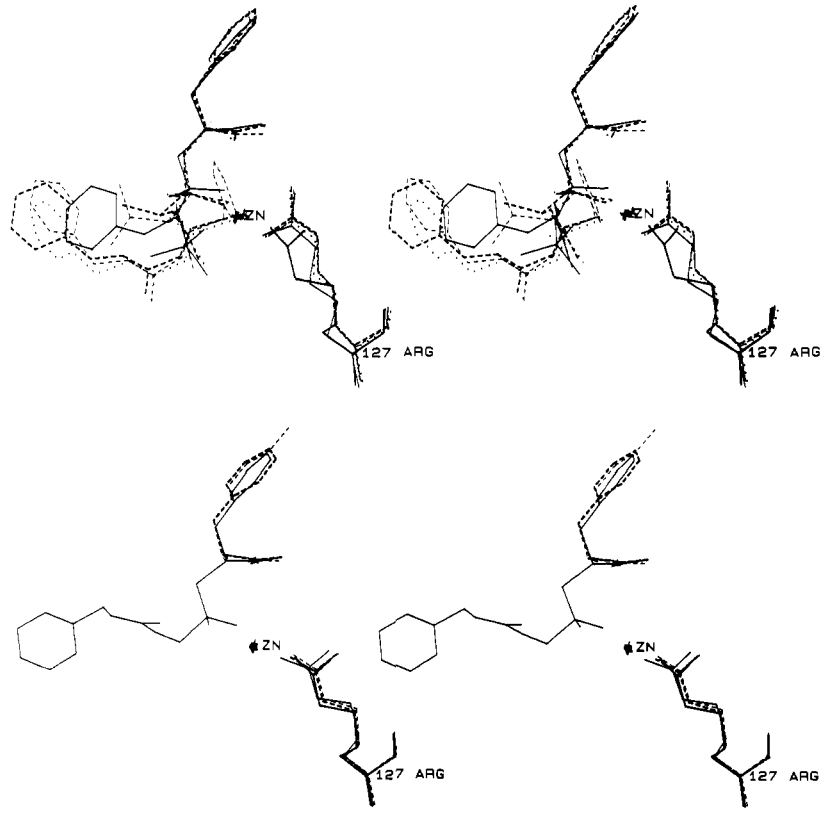

FIGURE 7: Stereoviews of the elongated (top) and coiled (bottom) conformations of the Arg-127 side chain in several CPA complexes and native CPA. Arg-127, the zinc, and the respective inhibitor are shown for each complex. The elongated (top) figure shows native CPA (thick solid lines), the CPA–hydrated ketomethylene complex (thin solid lines; Shoham et al., 1988), the CPA–ZAA^P(O)F complex (thick dashed lines; Kim & Lipscomb, 1990), the CPA–ZFV^P(O)F complex (thin dashed lines), and the CPA–ZAG^P(O)F complex (dotted lines). The C_α-chains of the CPA–ZAA^P(O)F, CPA–ZFV^P(O)F, and CPA–ZAG^P(O)F complexes were superimposed onto the C_α-chain of the CPA–hydrated ketomethylene complex. The CPA–hydrated ketomethylene complex is isomorphous with native CPA. The coiled (bottom) figure shows native CPA (thick solid lines), the CPA–phosphonamidate complex (thin solid lines; Christianson & Lipscomb, 1988), the CPA–D-Phe complex (thick dashed lines; Christianson et al., 1989), and the CPA–D-Tyr complex (thin dashed lines; Christianson et al., 1989). All of the structures shown in the coiled figure are isomorphous with each other.

ligands, including a phosphonamidate inhibitor, D-phenylalanine, and D-tyrosine (Christianson & Lipscomb, 1988; Jacobsen & Bartlett, 1981; Christianson et al., 1989). For these ligands, transition-state analogy has not been determined or is not appropriate. In the extended conformation, Arg-127 binds the carbonyl oxygen of the substrate, polarizing the scissile carbonyl for nucleophilic attack by Zn–hydroxyl (or Zn–water). Furthermore, by also binding the terminal carboxylate of the substrate, Arg-127 may help to stabilize the scissile bond in the proper orientation for hydrolysis. The aforementioned mutagenesis study showed that the Lys-127 mutant of rat carboxypeptidase A1 displays lower k_{cat} and higher K_m values for various peptide and ester substrates even though the electrophilic Lys-127 could also stabilize an oxyanionic intermediate. The functional difference between Arg-127 and Lys-127 is that the Arg-127 side chain can form two hydrogen bonds whereas the Lys-127 side chain can form only one. The second Arg-127 hydrogen bond was proposed to involve Asp-142 (Phillips et al., 1990). The Arg-127–Asp-142 interaction certainly is present, but the structures of these CPA–phosphonate complexes show that the second Arg-127 hydrogen bond more relevant to catalysis is likely the one involving the terminal carboxylate of the substrate. Although less dramatic than the native "up" to complex "down" conformational change seen in Tyr-248, the Arg-127 conformational change appears to be more selective since it is seen predominantly in those complexes involving transition-state or reaction-coordinate analogues. The apparent selectivity of this conformational change for productively bound ligands likely indicates the mechanistic importance of Arg-127.

ACKNOWLEDGMENTS

We gratefully acknowledge Prof. P. A. Bartlett for providing ZFV^P(O)F and ZAG^P(O)F. We thank Prof. P. A. Bartlett, along with Drs. S. K. Burley, J. E. Gouaux, and J.-Y. Liang, for excellent discussions.

REFERENCES

Abramowitz, N., Schechter, I., & Berger, A. (1967) *Biochem. Biophys. Res. Commun. 29*, 862–867.

Alexander, R. S., Kanyo, Z. F., Chirlian, L. E., & Christianson, D. W. (1990) *J. Am. Chem. Soc. 112*, 933–937.

Auld, D. S., & Vallee, B. L. (1970) *Biochemistry 9*, 602–609.

Auld, D. S., & Holmquist, B. (1974) *Biochemistry 13*, 4355–4361.

Auld, D. S., Galdes, A., Geoghegan, K. F., Holmquist, B., Martinelli, R. A., & Vallee, B. L. (1984) *Proc. Natl. Acad. Sci. U.S.A. 81*, 5041–5045.

Bartlett, P. A., & Marlowe, C. K. (1983) *Biochemistry 22*, 4618–4624.

Bartlett, P. A., & Marlowe, C. K. (1987) *Biochemistry 26*, 8553–8561.

Brünger, A. T. (1988) *X-PLOR Manual*, Version 1.5, Yale University, New Haven, CT.

Brünger, A. T., Kuriyan, J., & Karplus, M. (1987) *Science 235*, 458–460.

Burley, S. K., & Petsko, G. A. (1985) *Science 229*, 23–28.

Burley, S. K., & Petsko, G. A. (1986) *J. Am. Chem. Soc. 108*, 7995–8001.

Burley, S. K., & Petsko, G. A. (1988) *Adv. Protein Chem. 39*, 125–189.

Christianson, D. W., & Lipscomb, W. N. (1985) *Proc. Natl. Acad. Sci. U.S.A. 82*, 6840–6844.
Christianson, D. W., & Lipscomb, W. N. (1986) *Proc. Natl. Acad. Sci. U.S.A. 83*, 7568–7572.
Christianson, D. W., & Lipscomb, W. N. (1987) *J. Am. Chem. Soc. 109*, 5536–5538.
Christianson, D. W., & Lipscomb, W. N. (1988) *J. Am. Chem. Soc. 110*, 5560–5565.
Christianson, D. W., & Lipscomb, W. N. (1989) *Acc. Chem. Res. 22*, 62–69.
Christianson, D. W., David, P. R., & Lipscomb, W. N. (1987) *Proc. Natl. Acad. Sci. U.S.A. 84*, 1512–1515.
Christianson, D. W., Mangani, S., Shoham, G., & Lipscomb, W. N. (1989) *J. Biol. Chem. 264*, 12849–12853.
Copié, V., Kolbert, A. C., Drewry, D. H., Bartlett, P. A., Oas, T. G., & Griffin, R. G. (1990) *Biochemistry 29*, 9176–9184.
Davies, R. C., Riordan, J. F., Auld, D. S., & Vallee, B. L. (1968) *Biochemistry 7*, 1090–1099.
Fu, S.-C. J., Birnbaum, S. M., & Greenstein, J. P. (1954) *J. Am. Chem. Soc. 76*, 6054–6058.
Galdes, A., Auld, D. S., & Vallee, B. L. (1983) *Biochemistry 22*, 1888–1893.
Galdes, A., Auld, D. S., & Vallee, B. L. (1986) *Biochemistry 25*, 646–651.
Geoghegan, K. F., Galdes, A., Martinelli, R. A., Holmquist, B., Auld, D. S., & Vallee, B. L. (1983) *Biochemistry 22*, 2255–2262.
Geoghegan, K. F., Galdes, A., Hanson, G., Holmquist, B., Auld, D. S., & Vallee, B. L. (1986) *Biochemistry 25*, 4669–4674.
Green, N. M. (1963) *Biochem. J. 89*, 585–591.
Hanson, J. E., Kaplan, A. P., & Bartlett, P. A. (1989) *Biochemistry 28*, 6294–6305.
Hofmann, K., & Bergmann, M. (1940) *J. Biol. Chem. 134*, 225–235.
Holden, H. M., Tronrud, D. E., Monzingo, A. F., Weaver, L. H., & Matthews, B. W. (1987) *Biochemistry 26*, 8542–8553.
Izumiya, N., & Uchio, H. (1959) *J. Biochem. (Tokyo) 46*, 235–245.
Jacobsen, N. E., & Bartlett, P. A. (1981) *J. Am. Chem. Soc. 103*, 654–657.
Jones, T. A. (1982) in *Computational Crystallography* (Sayre, D., Ed.) pp 303–317, Clarendon Press, Oxford, England.
Kaplan, A. P., & Bartlett, P. A. (1991) *Biochemistry* (preceding paper in this issue).
Karlström, G., Linse, P., Wallqvist, A., & Jonssön, B. (1983) *J. Am. Chem. Soc. 105*, 3777–3782.
Kim, H., & Lipscomb, W. N. (1990) *Biochemistry 29*, 5546–5555.
Lee, B., & Richards, F. M. (1971) *J. Mol. Biol. 55*, 379–400.
Lienhard, G. (1973) *Science 180*, 149–154.
Lipscomb, W. N., Hartsuck, J. A., Reeke, G. N., Jr., Quiocho, F. A., Bethge, P. H., Ludwig, M. L., Steitz, T. A., Muirhead, H., & Coppola, J. (1968) *Brookhaven Symp. Biol. 21*, 24–90.
Machin, P. A. (1985) *Daresbury Lab. [Rep.] DL/SCI/R 23.*
Makinen, M. W., Kuo., L. C., Dymowski, J. J., & Jaffer, S. (1979) *J. Biol. Chem. 254*, 356–366.
Matthews, B. W. (1988) *Acc. Chem. Res. 21*, 333–340.
Nozaki, Y., & Tanford, C. (1971) *J. Mol. Biol. 246*, 2211–2217.
Pauling, L. (1948) *Nature 161*, 707–709.
Phillips, M. A., Fletterick, R., & Rutter, W. J. (1990) *J. Biol. Chem. 265*, 20692–20698.
Rees, D. C., & Lipscomb, W. N. (1982) *J. Mol. Biol. 160*, 475–498.
Rees, D. C., & Lipscomb, W. N. (1983) *Proc. Natl. Acad. Sci. U.S.A. 80*, 7151–7154.
Rees, D. C., Lewis, M., Honzatko, R. B., Lipscomb, W. N., & Hardman, K. D. (1981) *Proc. Natl. Acad. Sci. U.S.A. 78*, 3408–3412.
Rees, D. C., Lewis, M., & Lipscomb, W. N. (1983) *J. Mol. Biol. 168*, 367–387.
Shoham, G., Christianson, D. W., & Oren, D. A. (1988) *Proc. Natl. Acad. Sci. U.S.A. 85*, 684–688.
Snoke, J. E., & Neurath, H. (1949) *J. Biol. Chem. 181*, 789–802.
Tronrud, D. E., Monzingo, A. F., & Matthews, B. W. (1986) *Eur. J. Biochem. 157*, 261–268.
Wolfenden, R. (1976) *Annu. Rev. Biochem. Bioeng. 5*, 271–306.
Yanari, S., & Mitz, M. A. (1957) *J. Am. Chem. Soc. 79*, 1150–1158.